

# Wavelet-enabled Star Classification: A Deep Learning Approach for Identifying Binary and Exoplanet Stars

Aman Kumar,<sup>1</sup> and Sarvesh Gharat <sup>2</sup> 

<sup>1</sup>Tezpur University, Tezpur, Assam 784028, India.

<sup>2</sup>Centre for Machine Intelligence and Data Science, Indian Institute of Technology Bombay, 400076, Mumbai, India

arXiv:2301.13115v1 [astro-ph.IM] 30 Jan 2023

Accepted XXX. Received YYY; in original form ZZZ

## ABSTRACT

We present a novel approach for classifying stars as binary or exoplanet using deep learning techniques. Our method utilizes feature extraction, wavelet transformation, and a neural network on the light curves of stars to achieve high-accuracy results. We have also compiled a dataset of binary and exoplanet stars for training and validation by cross-matching observations from multiple space-based telescopes with catalogs of known binary and exoplanet stars. The application of wavelet transformation on the light curves has reduced the number of data points and improved the training time. Our algorithm has shown exceptional performance, with a test accuracy of 79.91%. This method can be applied to large datasets from current and future space-based telescopes, providing an efficient and accurate way of classifying stars.

**Key words:** methods: miscellaneous – methods: data analysis – (stars:) binaries: eclipsing

## 1 INTRODUCTION

The astronomical data is exploding as time passes and through the various instruments deployed by us, we are generating an enormous amount of data. One such instrument is *TESS*. The Transiting Exoplanet Survey Satellite (TESS) is a mission launched on April 18, 2018, whose goal is to discover earth-sized exoplanets orbiting the brightest dwarf stars (Ricker et al. 2015) (Barclay et al. 2018). TESS is equipped with four cameras, known as charge-coupled devices (CCDs), that can capture images of a region of the sky measuring 24 degrees by 96 degrees. The cameras will observe the brightness of 15,000 to 20,000 stars every 2 minute for a period of 27 to 356 days (Chrisp et al. 2015) (Fausnaugh et al. 2021). The data collected by TESS is processed at the Science Processing Operations Center (SPOC) and made available to the public in the form of Target Pixel Files (TPFs) and calibrated light curves (Jenkins et al. 2016), with a nominal cadence of 2 minutes for science data and 30 minutes for Full Frame Images (FFIs). TESS also maintains its own catalog of data, mostly observations of luminous objects taken by the satellite.

The Transiting Exoplanet Survey Satellite observes a variety of objects in the sky, ranging from stars to galaxies (Muirhead et al. 2018) (Guerrero et al. 2021). However, there is a need for rapid identification (Yu et al. 2019b) of these objects in the data as it is being generated. The primary target of observation for the TESS mission is stars, particularly host stars. The goal is to detect transits, which are the passing of planets between their host stars and us. These transits block a small amount of the star’s light as they pass by, thereby helping us to detect exoplanets. However, similar transits are also observed in the case of eclipsing binaries.

As discussed in (Ricker et al. 2015) (Sullivan et al. 2017), this can result in a large number of false positives, the majority of which are eclipsing binaries, which is a problem that needs to be addressed. Hence, classifying light curves that show transits into host stars and eclipsing binaries is a crucial task in astronomical studies, as both eclipsing binary systems and host stars are important objects (Jones et al. 2020) (Prša et al. 2022b) (Čokina et al. 2021) (Howell et al. 2021) (Campante et al. 2016) (Kane et al. 2020) (Campante et al. 2016) of study. The problem of classifying these time series data into binary categories is known as binary time series classification. Rapid identification of these objects is crucial in order to effectively analyze and interpret the data collected by TESS and other similar missions.

Given the recent trend of using machine learning to streamline the process of classification, we decide to employ a deep-learning model to classify the light curves in question. There have been several works in various fields that have used various deep learning models to classify time series data. For example, (Xu et al. 2019) uses a Long Short-term Memory (LSTM) based deep learning model to classify solar radio spectrum, and (Jamal & Bloom 2020) uses deep learning to classify variable stars. These studies demonstrate the potential of using deep learning models for time series classification and inspired us to investigate the use of deep learning for classifying TESS light curves. In addition to deep learning-based approaches, some works like (Dubath et al. 2011) have explored the use of traditional machine learning-based classification methods for similar tasks. These studies use various parameters, such as the period, amplitude, V-I color index, and absolute magnitude, to classify periodic variable stars using techniques like random forests. In summary, we present a method for classifying host stars and eclipsing binaries observed by TESS with high accuracy. This method utilizes both statistical

\* sarveshgharat19@gmail.com

parameters of the light curves and wavelet-transformed light curves as inputs to a deep learning model.

A wavelet transform, as described in literature such as (Chun-Lin 2010) and (Zhang & Zhang 2019), is a powerful mathematical tool utilized to analyze signals, such as time series data, in both the time and frequency domains (Rhif et al. 2019). The technique is based on the wavelet, which is a small, wave-like function that can be scaled and translated. The wavelet transform decomposes a signal into a series of wavelets, each of which represents a different frequency or scale. The resulting coefficients can be used to represent the signal in a more compact and efficient manner, and can also reveal features of the signal that may be difficult to detect in the original time series data. The use of wavelet transform in dimensionality reduction has been widely studied in the literature, as demonstrated in works such as (Keogh et al. 2001) and (Ukwatta & Wozniak 2015). The process involves using a technique such as Discrete Wavelet Transform (DWT) (Osadchiy et al. 2021) (Freire et al. 2019) (Al-Qerem et al. 2020) to decompose a signal into a series of detailed and approximation coefficients. The approximation coefficients are used to describe the overall trend of the signal, while the detailed coefficients provide information on the fine details of the signal. By keeping only the approximation coefficients and discarding the detailed coefficients, dimensionality reduction can be achieved while preserving the important features and variability of the original data.

Additionally, several works such as (Keogh et al. 2001), (Chakrabarti et al. 2002) and (Ukwatta & Wozniak 2015) have utilized the Discrete Wavelet Transform (DWT) for dimensionality reduction. This approach is effective in preserving the important features and inherent variability present in the signal while reducing the number of dimensions in the dataset. Therefore, in this context, DWT can be used to effectively reduce the dimensionality of light curves.

## 2 METHODOLOGY

### 2.1 Data Collection and Pre-Processing

The method being used for data processing and cleaning is similar to the one described in the paper "Exploring the TESS Eclipsing Binary stars" by (Pininti et al. 2023). The data sources being used are the VizieR Online Data Catalog: TESS Eclipsing Binary stars (Prsa et al. 2022a) and Exoplanet host stars (Su et al. 2022). The data is being cross-checked for observation through TESS and the associated FITS photo is being matched with the GAIA (Smart et al. 2021) (Prusti et al. 2016) (Brown et al. 2018) for validation of objects. This study uses 2-minute cadence SAP fluxes without any preprocessing. This approach is intended to make the study reliable for fast and rapid classification of objects without the need for extensive preprocessing and also to preserve the inherent features of the light curves. The data set includes 804 Host Star light curves and 787 Eclipsing Binary light curves, which have been cleaned for flagged data points and outliers beyond the 3 sigma range. It is important to note that the light curves have not been binned or folded, they were prepared in their original form for training the model.

Gaps in the TESS light curves are present due to various reasons, including spacecraft movement and telescope realignment. These

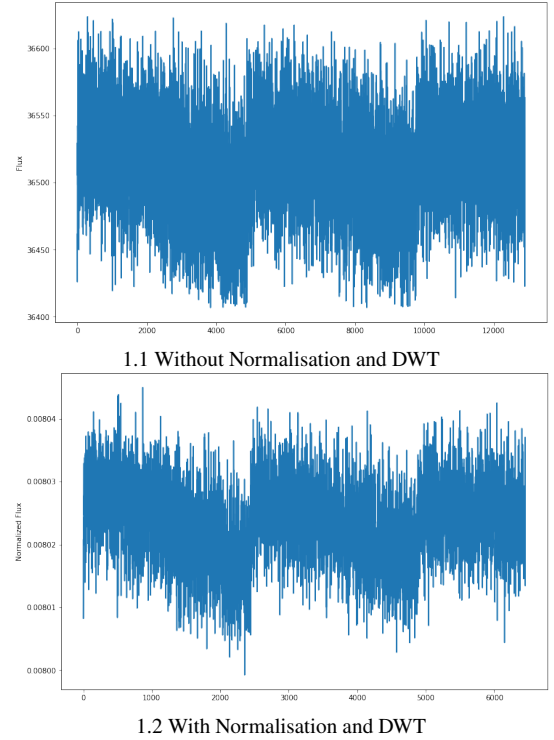
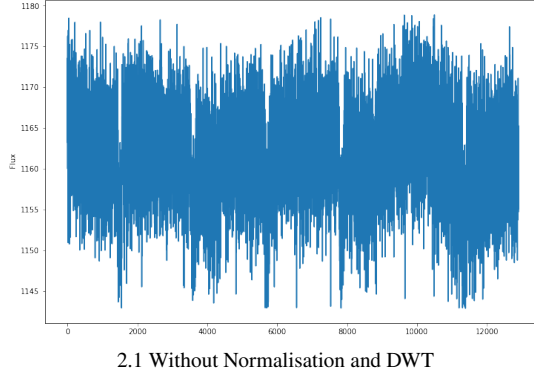
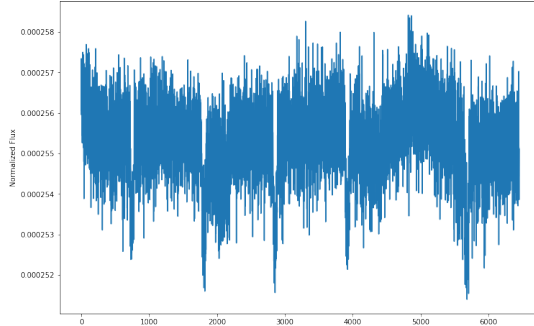


**Figure 1.** Sample lightcurve for class 0 (Eclipsing Binary)

gaps, which are random in nature and appear in different positions on various light curves, can be classified as systematic errors in the data (Pininti et al. 2023). To address this issue, we employed a method of stitching the light curves on both sides of the gap, effectively filling in the missing data and making the light curve more continuous (Hattori et al. 2022), thus improving the performance of our model. To ensure consistency in the dataset, the light curves were standardized to a length of 12901 data points, which was the length of the shortest light curve in the dataset. This was accomplished by removing data points from the end of the longer light curves. This standardization resulted in a minimal loss of data, as the longest light curve in the dataset was only 16007 data points in length. The light curves obtained through the previous process were then passed through a Discrete Wavelet Transform (DWT) to reduce their dimensions. We considered the approximation coefficients for our use as that's a low-pass filtered component of the original light curve. These coefficients represent a smoothed or less detailed version of the original signal. The low-pass filter is used to remove high-frequency components of the signal, which results in a smoothed version of the signal that contains mostly low-frequency information. The approximation coefficients can be thought of as a smooth version of the original signal, with the high-frequency details removed (Pathak 2009) (Sifuzzaman et al. 2009). The resulting light curves were 6455 data points in length. The DWT was performed using the PyWavelet Python package (Lee et al. 2019), and the "sym5" wavelet was utilized in this procedure. In addition to the light curves, we also calculated several statistical features, including the mean, standard deviation, variance, kurtosis, and skewness of each light curve, to serve as secondary inputs to our model. These parameters were calculated from the original light curves, prior to passing them through the DWT algorithm.



2.1 Without Normalisation and DWT



2.2 With Normalisation and DWT

Figure 2. Sample lightcurve for class 1 (Host Star)

## 2.2 Model Architecture

The proposed model is designed to accept two different types of inputs in order to improve both accuracy and generalization. To accomplish this, we included two separate input layers in the model, each accepting a different type of input. These inputs are then combined at a concatenation layer, allowing the model to utilize the information from both inputs.

We name these input layers as "parameter layer" and "lightcurve layer" based on the type of input they take in. The parameter layer takes in the statistical features calculated earlier, while the lightcurve layer takes in the time series data of the light curves after applying DWT.

### 2.2.1 Parameter Layer

The parameter layer takes in the statistical parameters calculated earlier as input, which is fed into a fully connected neural network. This network consists of 5 input neurons, connected to two fully connected layers with 500 units each. This architecture is commonly used in neural networks and has been shown to be effective in establishing a non-linear relationship between the input and output vector space in several studies such as (Khalifa et al. 2017), (Nieto et al. 2019), (Li et al. 2020). As with standard neural networks, each neuron in this layer is directly connected to all neurons in the layers below. To introduce non-linearity in the model, the ReLU activation function (Agarap 2018) (Ramachandran et al. 2017) is used in this layer, as it has been shown to be effective in deep learning architectures, as discussed in (Agarap 2018) and (Kulathunga et al. 2021). One of the major reasons behind the effective performance is its non-saturating

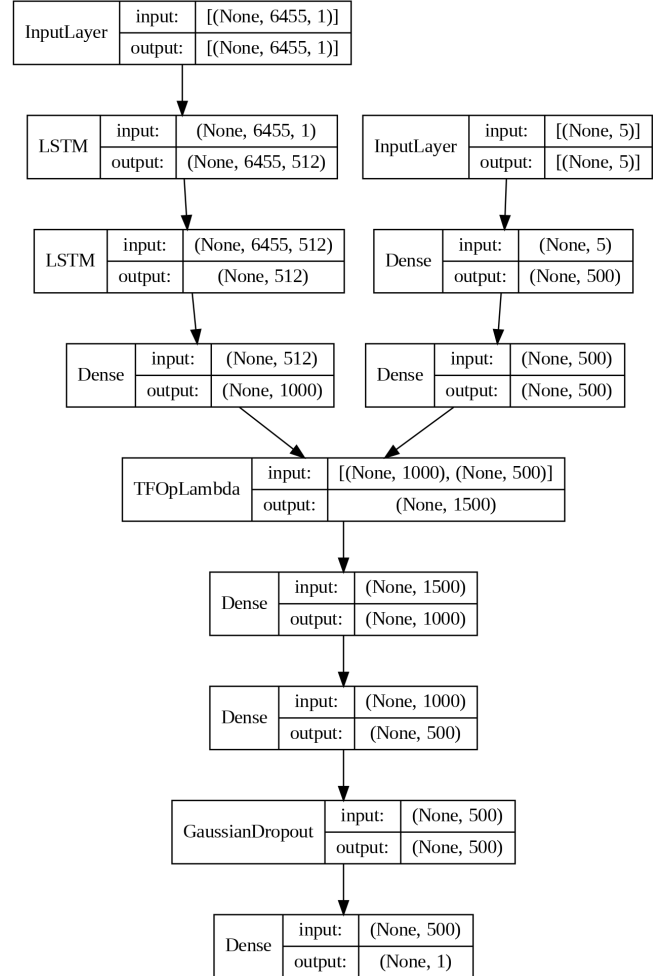


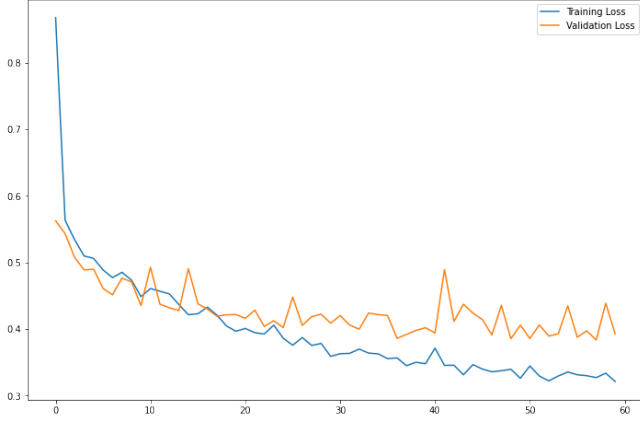
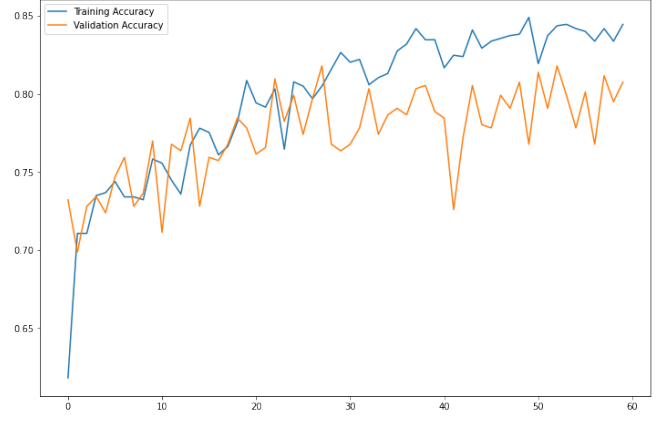
Figure 3. Model Architecture

ability along with the ability to allow the network to learn sparse representations.

### 2.2.2 LightCurve Layer

The light curve layer is an independent input layer that is introduced to regularize the model and extract the inherent features of the light curves that the statistical parameters cannot capture. This layer is made up of LSTM units, which are known for their exceptional performance when it comes to sequential inputs (Staudemeyer & Morris 2019a) such as time series data. Unlike their predecessors, RNNs, LSTMs have the property of long-term memory, which helps them to relate data points of a sequence over a longer duration, as discussed in studies such as (Yu et al. 2019a) and (Smagulova & James 2019). RNNs can only gaze back in time for a maximum of 10 timesteps (Staudemeyer & Morris 2019b). This is because the signal being given back are either vanishing or exploding. Long-Short Term Memory Recurrent Neural Networks were developed to overcome this issue (LSTM-RNN) (Mozer 1991) (Hochreiter 1991).

In the proposed model, we use an LSTM layer with 512 units that takes light curves as an input and generates a secondary sequence, which is then passed on to another set of 512 LSTM units. This is connected to a fully connected layer of 1000 units.

**Figure 4.** Model Loss vs Epochs**Figure 5.** Model Accuracy vs Epochs

### 2.2.3 Concatenation Layer

The concatenation layer combines both the parameter layer and the lightcurve layer. It connects them to a fully connected layer of 1000 units, which is then connected to a layer with 500 units. This is followed by a Gaussian Dropout (Srivastava et al. 2014) with a dropout rate of 0.2. The Gaussian dropout is a regularization technique that aims to prevent over-fitting and improves generalization by randomly dropping out network connections. This increases the training time but results in better generalization and prevents over-fitting (Srivastava et al. 2014). The dropout layer then connects to the output layer, which has a single unit activated by a sigmoid (Narayan 1997) function. This allows the output layer to produce a result between 0 and 1 which also represents the probability of the prediction.

### 2.3 Training and Validation

The proposed model is implemented using TensorFlow (Abadi et al. 2015) and trained on Google Collaboratory utilizing an NVIDIA K80 GPU (Carneiro et al. 2018). The dataset is divided into a 70 : 30 ratio, with 70% of the data used for training and 30% used for validation and testing. The inclusion of validation data is essential for tuning the hyper-parameters of the model. The training was conducted over 100 epochs, with a stopping condition implemented to prevent overfitting (Caruana et al. 2001) (Song et al. 2019) (Ying 2019). As depicted in Figure 5, the training accuracy continuously increases, however, the validation accuracy reaches a saturation point and begins to oscillate. Therefore, the inclusion of a stopping condition not only reduces computational requirements but also minimizes the risk of overfitting.

In order to optimize the model, we choose to use Adam (Kingma & Ba 2014) as an optimizer, which is known for its robustness to noise and adaptive learning rate properties. Additionally, being a momentum-based optimizer, Adam is a popular choice among practitioners in the field of deep learning. Furthermore, since our model is designed for binary classification, the use of Binary Cross Entropy as the loss function is appropriate. The learning and decay rate of the optimizer has been fine-tuned to be  $10^{-4}$  through a process of experimentation with various permutations and combinations within a similar range.

**Table 1.** Confusion Matrix

|         | Class 0 | Class 1 |
|---------|---------|---------|
| Class 0 | 176     | 69      |
| Class 1 | 23      | 210     |

## 3 RESULTS

The proposed study consists of a wavelet-enabled star classifier making use of Deep Learning to classify exoplanets and binary stars. The proposed model makes a correct prediction with an accuracy of 79.91%. To calculate accuracy, we make use of the confusion matrix shown in Table 1.

The other metric to test the performance of the model is the F1 score. To calculate F1 score, we make use of.

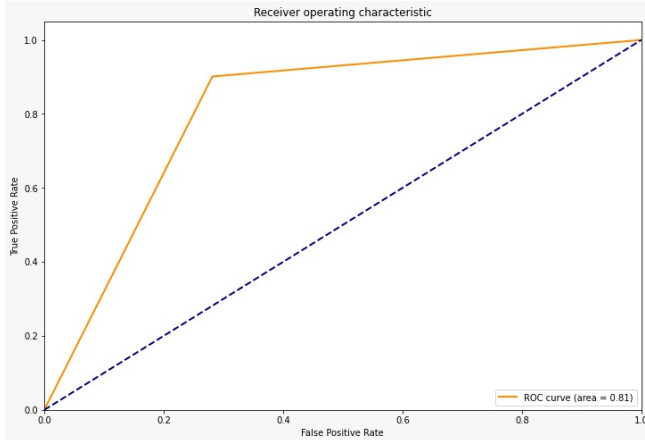
$$F1 = \frac{2PR}{P+R}$$

Here,  $P$  and  $R$  represent precision and recall respectively. Precision in general represents the false positive rate i.e. precision of class 0 will tell about the data misclassified as class 0. Similarly, Recall represents the false negative rate. All these parameters are bounded in the region 0 to 1. Ideally, the more the value of the parameter is, the better the algorithm is. As seen from Table 2, the recall corresponding to class 0 is comparatively less than that of class 1, which means relatively more exoplanets are predicted as eclipsing binaries as opposed to binaries being predicted as exoplanets. One advantage of the F1 score over accuracy is that it is more sensitive to imbalanced datasets, where accuracy can be misleading. For example, if a model always predicts the majority class, it may have a high accuracy even though it is not correctly identifying the minority class. The F1 score, on the other hand, will be lower in this scenario. Another advantage is that the F1 score is able to balance the trade-off between precision and recall. In some applications, it is more important to have a high recall (i.e. minimize false negatives) while in others it is more important to have a high precision (i.e. minimize false positives). The F1 score takes into account both of these factors, making it a more comprehensive measure of model performance.

Additionally, when it comes to "Binary Classification", the ROC curve happens to be a graphical representation of the algorithm's

**Table 2.** Precision, Recall and F1 score

| Class   | Precision | Recall | F1 score |
|---------|-----------|--------|----------|
| Class 0 | 0.88      | 0.72   | 0.79     |
| Class 1 | 0.75      | 0.90   | 0.82     |
| Average | 0.81      | 0.81   | 0.80     |

**Figure 6.** ROC curve

performance. It plots the true positive rate against the false positive rate at different classification thresholds. The area under the ROC curve (AUC) is a metric that summarizes the overall performance of the classifier. The ROC curve is important in classification tasks because it allows us to visualize the trade-off between the true positive rate and the false positive rate and choose an appropriate threshold for the classifier. Additionally, AUC provides a single-number summary of the classifier performance.

As seen from Figure 6 the AUC value by the proposed model is 0.81. In an ideal case, the value of AUC needs to be 1. ROC curves have an attractive property i.e they are insensitive to changes in class distribution. If the proportion of positive to negative instances changes in a test set, the ROC curves won't change as opposed to what happens in the case of accuracy.

## 4 CONCLUSION

The current study employs a wavelet-enabled Long Short-Term Memory (LSTM) model in combination with key statistical features to classify binary eclipses and exoplanet stars. A significant advantage of our algorithm is its ability to make predictions using solely light curve data. In many instances, the classification of similar transits can prove challenging. However, our approach effectively addresses this challenge through the careful selection of the feature space. The achieved "accuracy" in our case happens to be 79.91% with an average "F1" score of 0.80. These numbers happen to be a significant advancement in the classification process considering the high similarity in the light curve data resulting in multiple challenges in identifying the feature space.

## ACKNOWLEDGEMENTS

This research uses Lightkurve, a Python package for analyzing Kepler and TESS data (Collaboration et al. 2018). The TESS mission is funded by the Science Mission directorate of NASA. This study utilized ASTROPY, a community-developed Python core package for astronomy (Price-Whelan et al. 2018). This study also employed astroquery, a Python package for astronomical web-querying (Ginsburg et al. 2019).

## DATA AVAILABILITY

The paper contains TESS mission data that are publically accessible from the Mikulski Archive for Space Telescopes (MAST). The data and code used can be found here <https://github.com/amanasci/hs-eb-classification>

## REFERENCES

Abadi M., et al., 2015, TensorFlow: Large-Scale Machine Learning on Heterogeneous Systems, <https://www.tensorflow.org/>

Agarap A. F., 2018, arXiv preprint arXiv:1803.08375

Al-Qerem A., Kharbat F., Nashwan S., Ashraf S., Blaou K., 2020, International Journal of Distributed Sensor Networks, 16, 1550147720911009

Barclay T., Pepper J., Quintana E. V., 2018, The Astrophysical Journal Supplement Series, 239, 2

Brown A., et al., 2018, Astronomy & astrophysics, 616, A1

Campante T., et al., 2016, The Astrophysical Journal, 830, 138

Carneiro T., Da Nóbrega R. V. M., Nepomuceno T., Bian G.-B., De Albuquerque V. H. C., Reboucas Filho P. P., 2018, IEEE Access, 6, 61677

Caruana R., Lawrence S., Giles L., 2001, in Proceedings of the 2000 Conference, Vancouver, BC, Canada. pp 3–8

Chakrabarti K., Keogh E., Mehrotra S., Pazzani M., 2002, ACM Transactions on Database Systems (TODS), 27, 188

Chrisp M., Clark K., Primeau B., Dalpiaz M., Lennon J., 2015, in UV/Optical/IR Space Telescopes and Instruments: Innovative Technologies and Concepts VII. pp 129–135

Chun-Lin L., 2010, NTUEE, Taiwan, 21, 22

Čokina M., Maslej-Krešnáková V., Butka P., Parimucha Š., 2021, Astronomy and Computing, 36, 100488

Collaboration L., et al., 2018, Astrophysics Source Code Library (ascl: 1812.013)

Dubath P., et al., 2011, Monthly Notices of the Royal Astronomical Society, 414, 2602

Fausnaugh M., et al., 2021, Publications of the Astronomical Society of the Pacific, 133, 095002

Freire P. K. d. M. M., Santos C. A. G., da Silva G. B. L., 2019, Applied Soft Computing, 80, 494

Ginsburg A., et al., 2019, The Astronomical Journal, 157, 98

Guerrero N. M., et al., 2021, The Astrophysical Journal Supplement Series, 254, 39

Hattori S., Foreman-Mackey D., Hogg D. W., Montet B. T., Angus R., Pritchard T., Curtis J. L., Schölkopf B., 2022, The Astronomical Journal, 163, 284

Hochreiter S., 1991, Diploma, Technische Universität München, 91

Howell S. B., Matson R. A., Ciardi D. R., Everett M. E., Livingston J. H., Scott N. J., Horch E. P., Winn J. N., 2021, The Astronomical Journal, 161, 164

Jamal S., Bloom J. S., 2020, The Astrophysical Journal Supplement Series, 250, 30

Jenkins J. M., et al., 2016, in Software and Cyberinfrastructure for Astronomy IV. pp 1232–1251

Jones D., et al., 2020, The Astrophysical Journal Supplement Series, 247, 63

Kane S. R., et al., 2020, Publications of the Astronomical Society of the Pacific, 133, 014402

Keogh E., Chakrabarti K., Pazzani M., Mehrotra S., 2001, Knowledge and information Systems, 3, 263

Khalifa N. E. M., Taha M. H. N., Hassanien A. E., Selim I., 2017, arXiv preprint arXiv:1709.02245

Kingma D. P., Ba J., 2014, arXiv preprint arXiv:1412.6980

Kulathunga N., Ranasinghe N. R., Vrinceanu D., Kinsman Z., Huang L., Wang Y., 2021, Algorithms, 14, 51

Lee G., Gommers R., Waselewski F., Wohlfahrt K., O'Leary A., 2019, Journal of Open Source Software, 4, 1237

Li X., Zheng Y., Wang X., Wang L., 2020, The Astrophysical Journal, 891, 10

Mozer M. C., 1991, Advances in neural information processing systems, 4

Muirhead P. S., Dressing C. D., Mann A. W., Rojas-Ayala B., Lépine S., Paegert M., De Lee N., Oelkers R., 2018, The Astronomical Journal, 155, 180

Narayan S., 1997, Information sciences, 99, 69

Nieto D., Brill A., Feng Q., Humensky T., Kim B., Miener T., Mukherjee R., Sevilla J., 2019, arXiv preprint arXiv:1912.09877

Osadchiy A., Kamenev A., Saharov V., Chernyi S., 2021, Designs, 5, 41

Pathak R. S., 2009, The wavelet transform. Springer Science & Business Media

Pininti V. R., Bhatta G., Paul S., Kumar A., Rajgor A., Barnwal R., Gharat S., 2023, Monthly Notices of the Royal Astronomical Society, 518, 1459

Price-Whelan A. M., et al., 2018, The Astronomical Journal, 156, 123

Prsa A., et al., 2022a, VizieR Online Data Catalog, pp J-ApJS

Prša A., et al., 2022b, The Astrophysical Journal Supplement Series, 258, 16

Prusti T., et al., 2016, Astronomy & astrophysics, 595, A1

Ramachandran P., Zoph B., Le Q. V., 2017, arXiv preprint arXiv:1710.05941

Rhif M., Ben Abbes A., Farah I. R., Martínez B., Sang Y., 2019, Applied Sciences, 9, 1345

Ricker G. R., et al., 2015, Journal of Astronomical Telescopes, Instruments, and Systems, 1, 014003

Sifuzzaman M., Islam M., Ali M., 2009, Journal of Physical Sciences, 13, 121

Smagulova K., James A. P., 2019, The European Physical Journal Special Topics, 228, 2313

Smart R. L., et al., 2021, Astronomy & Astrophysics, 649, A6

Song H., Kim M., Park D., Lee J.-G., 2019, arXiv preprint arXiv:1911.08059

Srivastava N., Hinton G., Krizhevsky A., Sutskever I., Salakhutdinov R., 2014, The journal of machine learning research, 15, 1929

Staudemeyer R. C., Morris E. R., 2019a, arXiv preprint arXiv:1909.09586

Staudemeyer R. C., Morris E. R., 2019b, CoRR, abs/1909.09586

Su T., et al., 2022, VizieR Online Data Catalog, pp J-ApJS

Sullivan P. W., et al., 2017, The Astrophysical Journal, 837, 2pp

Ukwatta T. N., Wozniak P. R., 2015, in 2015 IEEE Applied Imagery Pattern Recognition Workshop (AIPR). pp 1–10

Xu L., Yan Y.-H., Yu X.-X., Zhang W.-Q., Chen J., Duan L.-Y., 2019, Research in Astronomy and Astrophysics, 19, 135

Ying X., 2019, in Journal of physics: Conference series. p. 022022

Yu Y., Si X., Hu C., Zhang J., 2019a, Neural computation, 31, 1235

Yu L., et al., 2019b, The Astronomical Journal, 158, 25

Zhang D., Zhang D., 2019, Fundamentals of Image Data Mining: Analysis, Features, Classification and Retrieval, pp 35–44

This paper has been typeset from a  $\text{\TeX}$ / $\text{\LaTeX}$  file prepared by the author.